Available online at https://sej.journals.ekb.eg/

FACULTY OF ENGINEERING – SOHAG UNIVERSITY

SOHAG ENGINEERING JOURNAL (SEJ), VOL. 1, NO. 1, MARCH 2021

SELECTING TRAINING SAMPLES AUTOMATICALLY FROM VHR SATELLITE IMAGES FOR IMAGE CLASSIFICATION

Mohamed Fawzy[a*], Farag Khodary[a], and Yasser G. Mostafa[b]

[a]*Civil Eng. Dept., Faculty of Engineering, South Valley University, Qena, Egypt*
[b] *Civil Eng. Dept., Faculty of Engineering, Sohag University, Sohag, Egypt*

Abstract

Classification is one of the most significant phases for remote sensing image interpretation. All the supervised classifiers need sufficient and efficient training samples, which are usually selected manually and labeled by visual inspection or field survey. Selecting training samples manually requires more time and human effort. A new method is proposed for automatic selection of training samples from a Very High Resolution (VHR) satellite image. The proposed method is tested for selecting training samples automatically for standard supervised pixel-based classification methods instead of manual samples selection. The proposed method uses a set of indices with specific thresholds to identify the training areas for each class. A certain part of each index histogram can be chosen for each class and consider as training samples. Automatic training samples are compared with manual samples for three standard classification methods. The average accuracy achieved by the proposed automatic sample selection is promising; 76.56% for maximum likelihood classifier, 74.06% for spectral correlation mapper classifier, and 70.00% for spectral angle mapper classifier. Although their accuracy scores are slightly nearby classification with manually selected samples by an average of 1.74% for maximum likelihood, 2.44% for spectral correlation mapper, and 3.75% for spectral angle mapper classifier.

 DOI: 10.21608/SEJ.2021.155929.

Keywords: Feature extraction; images classification; training samples; worldview-2.

1. INTRODUCTION

Urban land cover classification using Very High Resolution (VHR) satellite images is the most important source of information for urban areas mapping. Classification is one of the most significant phases for remote sensing image interpretation. Supervised classification is the commonly used method for feature extraction from images and it requires selecting training samples. Classification results depend mainly on training samples selection. Manually selection of training samples is a time-consuming task, expensive and depends mainly on the analyst. Automatic selection of training samples is a challenging task [1]. Pixels that represent patterns or land cover features are identified from other sources, such as aerial photos, filed survey, or maps. By identifying these patterns, the pixels with similar characteristics can be identified [2].

Various methods of supervised classification have been applied to remote sensing classification like, Maximum likelihood, Spectral correlation mapper, and Spectral angle mapper. Efficient training samples are needed in the supervised classifiers presented. They are frequently selected and labeled by visual inspection or field survey. Most supervised classification algorithms can produce high classification accuracies if the

* Corresponding author: Mohamedfawzy@eng.svu.edu.eg

parameters are properly set, and training samples are appropriately representative. less representative training samples decreased accuracy of supervised algorithm results [3].

The implementation of the training stage is based on the classifier used since individual training cases can vary in value. For example, the maximum likelihood classifier uses parameters such as the mean and covariance matrix that summarize the spectral response of each class while a multilayer perceptron neural network uses each training case directly [4]. A training set that can be used to derive a highly accurate classification from one classifier may yield a significantly lower accuracy if used with another classifier [5]. It can be observed that training samples should be correct, pure, representative, and uniformly distributed in the whole image. When sufficiently representative training samples are used, results of classification are improved [3]. The training sets are used as references for the classification of other pixels in the image. However, the accuracy of this classification is highly dependent on the number of training sets that were used [6].

It is recommended that the number of training samples (n) for each class should not be fewer than 10–30 times the number of bands (P). To ensure that n be comprised of at least 10 to 30 times the number of discriminating wavebands (i.e., n=10p to 30p). Most likely this n-to-p relationship was originally intended to be a "rule of thumb", but for most, has turned into a general rule to be applied universally [7]. Although using the minimum training samples achieves adequate results when the analyst uses a larger number better results can be obtained. Moreover, it is typically argued that the bigger the training set the better precision of the estimates made [4].

The main objective of this research is to represent an automatic method for training samples selection from VHR satellite images for image classification. The remainder of this paper is organized as follows. Section 2 represents the methodology. Section 3 describes the data used and image preprocessing. Proposed samples selection method is described in Section 4. Results and discussions are explained in Section 5. Finally, conclusions are illustrated in Section 6.

2. METHODOLOGY

In order to automatically collect reliable training samples, a series of processing steps are proposed to select, refine, and test samples that are directly extracted from the indices. The process is achieved through five stages (Fig. 1). First, a suitable index to detect pixels of each informational class is selected. Second, training samples on the histogram for each class are identifying. Third, training samples are refined and tested. Fourth, signatures (mean, standard deviation, variance, covariance, etc.) are identified. Finally, classification is carried out using the proposed method.

Indices are used in consecutive order for features extraction. Indices are chosen based on WorldView-2 bands. Water and vegetation classes have been the first focus of normalized index ratios because it is easy to identify by the difference in reflectance values. Then, bare soil class is extracted, as a natural class and isolated from the rest man made classes, buildings, and roads. Finally, buildings and roads can be identified and separated by wavelength absorption features associated with mineral composition or other material properties.

3. DATA USED AND IMAGE PREPROCESSING

Qena governorate has various urban areas with different degrees of planning. For this work, a WorldView-2 (WV-2) satellite image with eight spectral bands, captured in March 2017, is used. Four study areas were chosen with different Characteristics (Fig.2). Study areas A and B represent semi planned areas. Study area C represents unplanned area. Study area D represents a rural village. They have various land cover such as water, vegetation, bare soil, buildings, and roads (Fig.3).

Data pre-processing is essential to better interpretation and extract the maximum information from satellite images [8]. In this paper, image preprocessing was applied through three steps: data fusion, geo-referencing, and shadow correction. The Data fusion process was performed using Principles Component Analysis (PCA) to keep the number of bands the same before and after merge [9]. Shadow correction technique was applied to compensate the brightness difference between shadow and non-shadow areas through two main steps: shadow detection and compensation. Shadow detection is carried out using Optimized Shadow Index (OSI) proposed by [10]. Shadow compensation is carried using Linear Correlation Correction (LCC) method [11]. The geometric correction process was applied using the third-order polynomial transformation method using (16) GCPs to rectify WorldView-2 satellite image to Egyptian Transverse Mercator (ETM) projection. The image was rectified

with Root Mean Square (RMS) error in the checkpoints as 0.65 m. The resampling process was carried out by using the nearest neighbor method to avoid smoothing the original image data.

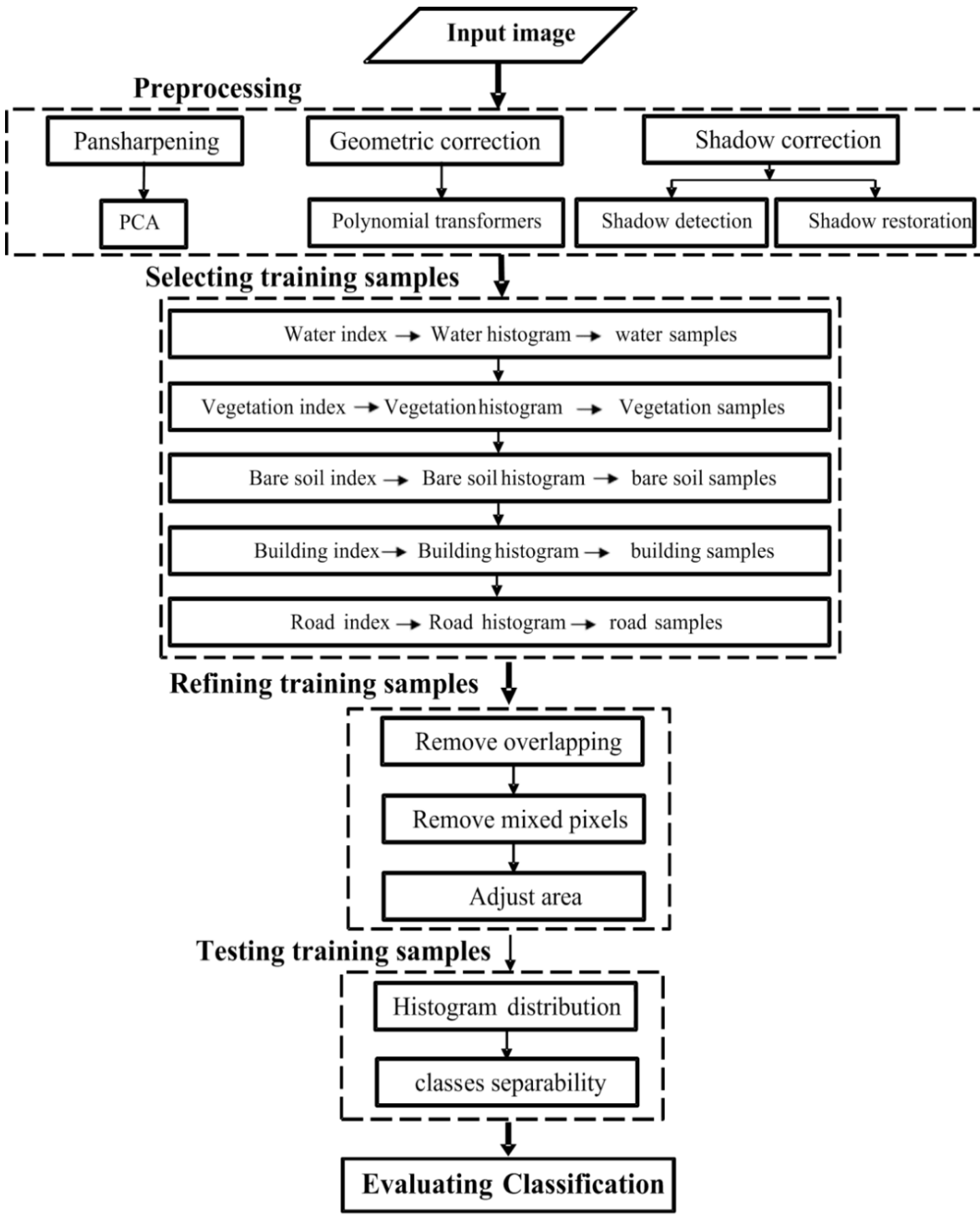

Fig. 1. Steps of selecting, refining, and testing samples automatically.

Fig. 2. WorldView-2 image for Qena city-Egypt.

Fig. 3. Four used study areas A, B, C, and D.

4. PROPOSED SAMPLES SELECTION METHOD

Indices have achieved satisfactory results for indicating different land cover classes and can be used to develop an automatic method for selecting training samples instead of manual selection. A new method is proposed for automatic selection of training samples from Very High Resolution (VHR) satellite images. The most suitable indices for different classes in the Egyptian environment are tested and compared. Then the most suitable index is chosen for each class. Normalized Difference Water Index (NDWI), Modified Normalized Difference Water Index (MNDWI), and World View Water Index (WV-WI) were compared to identify water. Normalized Difference Vegetation Index (NDVI), World View Normalized Difference Vegetation Index (WV-NDVI), and World View Vegetation Index (WV-VI) were compared to identify vegetation. Soil Adjusted Vegetation Index (SAVI), Modified Soil Adjusted Vegetation Index (MSAVI2), and World View Soil Index (WV-SI) were compared to identify bare soil. World View Building Index (WV-BI), and Building Spectral Index (BSI) were compared to identify buildings. Road Extraction Index (REI) is chosen to identify roads [8]. For the proposed method, MNDWI for water, WV-VI for vegetation, SAVI for bare soil, WV-BI for buildings, and REI for roads are used in consecutive order.

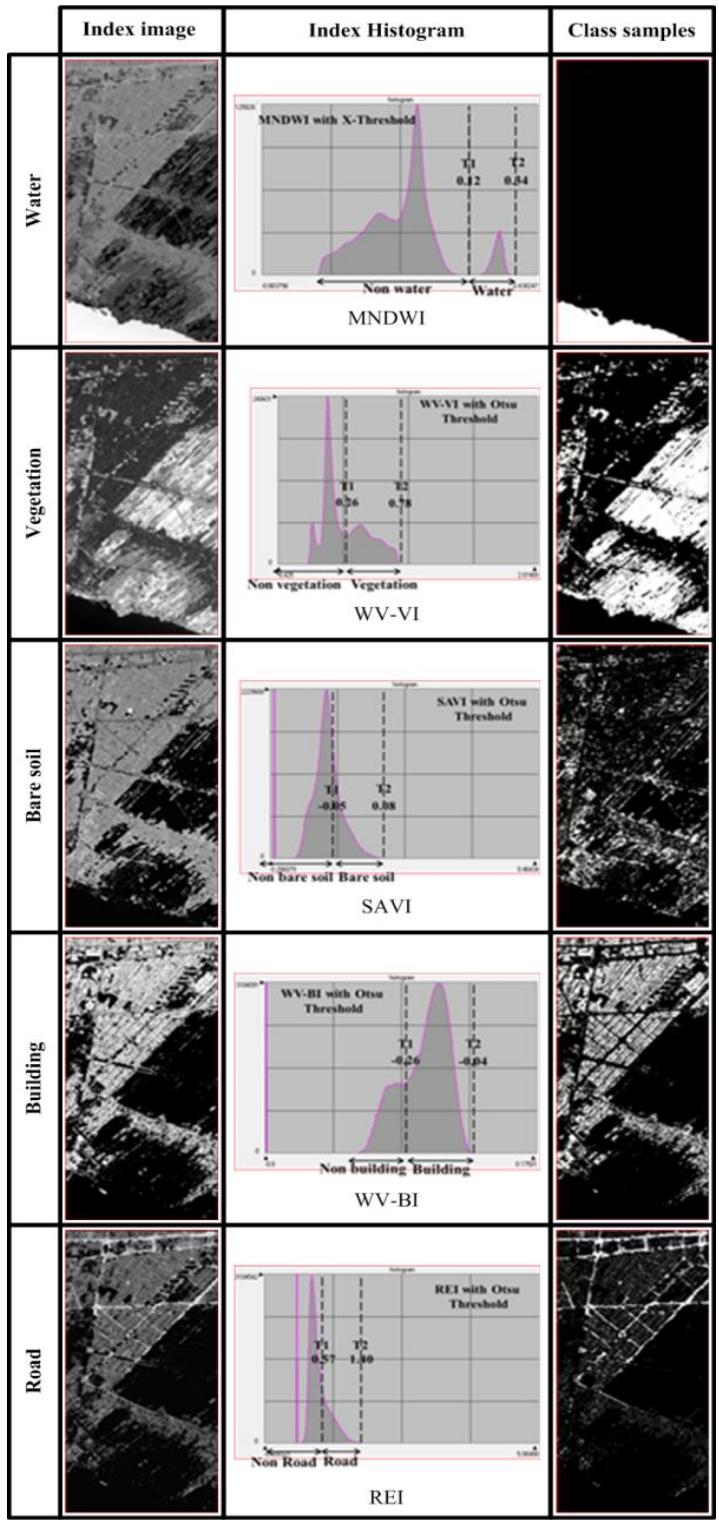

Fig. 4. Indices images, histograms, and samples for water, vegetation, bare soil, buildings, and roads of study area A.

A certain part of each index histogram can be chosen for each class and consider as training samples. This part locates between two thresholds T1 and T2. They can be extracted using a suitable threshold method. They

depend on the position of chosen class on the histogram. X-Threshold is used for water extraction to separate non-shadow, shadow, and water areas automatically [10]. For class identification, T1 can be chosen from X threshold or Otsu threshold, while T2 is chosen at the end of histogram. Otsu threshold is used with other classes as it's one of the better threshold selection methods for general real world images with regard to uniformity and shape measures [12]. It is based on an analysis of the histogram of the tonal image resulting from the selected index image calculation. The histograms representing two normal intensity distributions, one representing foreground and the remainder representing the background. Fig. 4 shows histograms, indices images, and samples selected for study areas A.

4.1. Refining Training Samples

Refinement operations are important to shift focus towards the purest exemplars of the classes, which may often be considered to be end members [4]. Some problems affect samples selection such as overlapping between similar classes, mixed pixels between two classes, and insufficient areas for classification. In this work, choosing samples from indices in consecutive order prevents overlapping between similar classes (i.e., building, road, and bare soil). Considering the difficulty and uncertainty in labeling samples in mixed pixels regions, the samples that are labeled as more than one class are removed, and the extracted training samples are adjusted to the suitable area to meet the requirements of training samples.

4.2. Testing Training Samples

For each spectral class, the chosen samples are tested using the tools available in the imaging processing system. Assess uniformity of the histogram, class separability as revealed by the divergence matrix, and their visual appearance on the image [13].

4.2.1. Histogram Distribution

After the training samples are established, each training sample 'signature' is scrutinized by looking at the brightness count histogram for each band of each sample. It is checked to determine if the sample had a unimodal or bimodal distribution for its brightness signature. A unimodal distribution indicates that the reflectance values for the training sample likely comes from one type of land feature, such as urban or water (Fig. 5). The histogram should exhibit a unimodal distribution in each band. A bimodal distribution would be evidence that the training sample had two distinct classes of pixels instead of one classification (i.e., a region being picked to train pixels of building region may include some road area also). Training sets that failed in this test were deleted and replaced [14].

4.2.2. Classes Separability

The spectral classes produced by the training sites must be sufficiently separate in order to enable the classifier to differentiate between the various class signatures. If the class separabilities are too low, then this will lead to a high number of misclassified pixels. Signature separability is a statistical measure of distance between two signatures. The class separabilities for the training and verification sites are calculated using the Jeffries-Matusita separability measures (Eq. (2)). These values range from 0 to 1414 and indicate how well the selected sites are statistically separate [15]. The higher value means good separabilities. The formula for computing Jeffries-Matusita Distance (JM) is as follows:

$$\alpha = \frac{1}{8}\left(\mu_i - \mu_j\right)^T \left(\frac{C_i + C_j}{2}\right)^{-1} \left(\mu_i - \mu_j\right) + \frac{1}{2} ln \left(\frac{|(C_i + C_j)/2|}{\sqrt{|C_i| \times |C_j|}} \right) \quad (1)$$

$$JM_{ij} = \sqrt{2(1 - e^{-\alpha})} \quad (2)$$

where i and j are the two signatures (classes) being compared, C_i and C_j are the covariance matrix of signatures i and j, respectively, μ_i and μ_j are the mean vectors of signatures i and j, respectively, $|C_i|$ and $|C_j|$ are the determinant of C_i and C_j (matrix algebra), respectively.

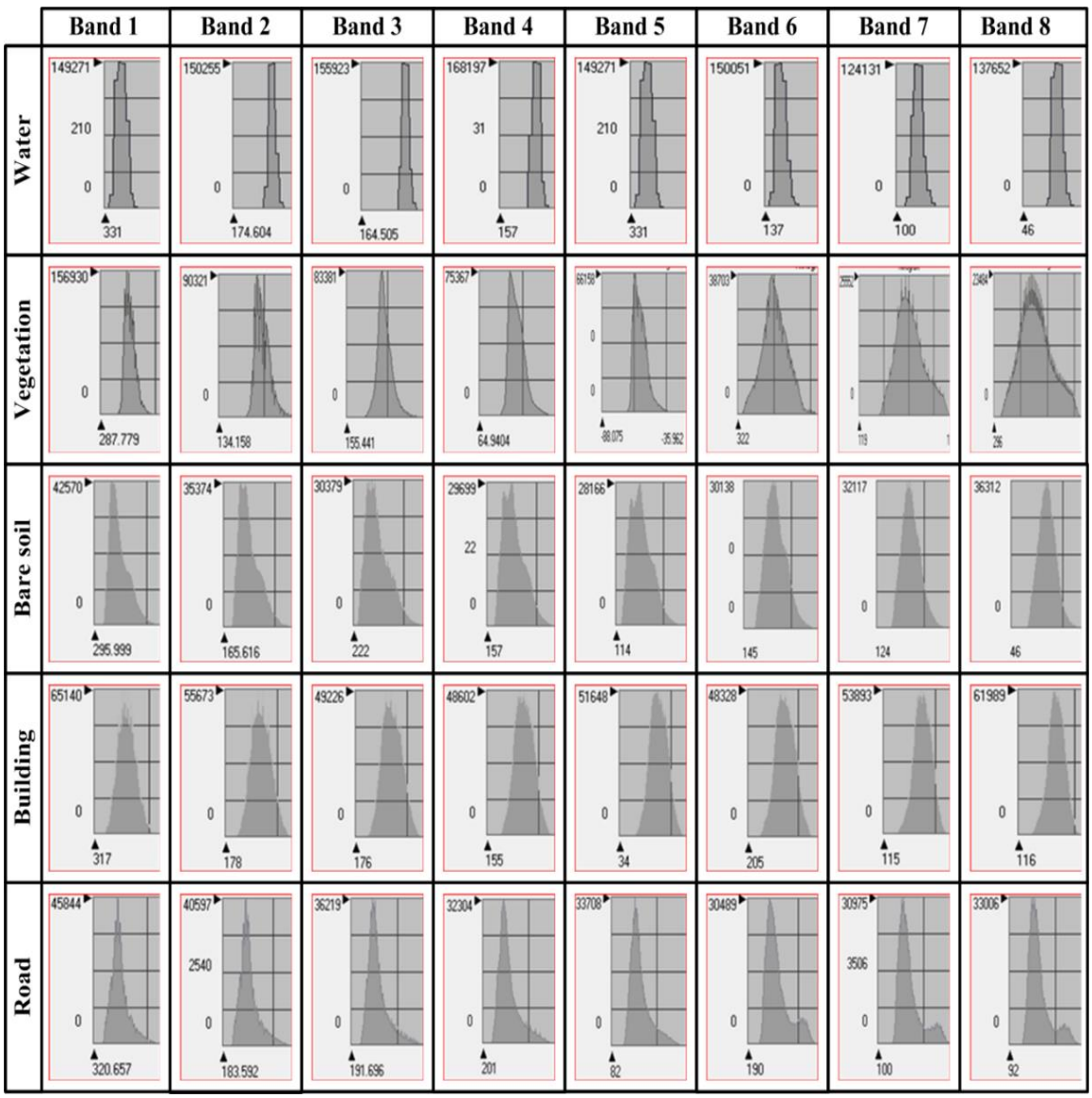

Fig. 5. Histograms distribution of eight bands for different classes samples

Results shown in Table 1 present separabilities testing values for both manual and automatic selected training samples of study areas A, B, C, and D.

TABLE 1. CLASSES SEPARABILITY TESTING OF STUDY AREAS A, B, C AND D.

Study area		Class Pairs										Min	Max	Avg
		W:V	W:BS	W:B	W:R	V:BS	V:B	V:R	BS:B	BS:R	B:R			
A	Manual	1414	1414	1414	1414	1414	1414	1412	1366	1413	1396	1366	1414	1407
	20%	1414	1414	1414	1414	1396	1414	1414	1378	1321	1127	1127	1414	1371
	50%	1414	1347	1413	1406	1414	1414	1414	1321	1236	1023	1023	1414	1340
	100%	1414	1414	1414	1413	1229	1363	1355	1118	1055	809	809	1414	1260
B	Manual	1414	1414	1414	1413	1414	1414	1414	1398	1414	1398	1398	1414	1411
	20%	1414	1414	1414	1411	1382	1414	1413	1391	1201	1342	1201	1414	1360
	50%	1414	1413	1414	1407	1327	1412	1397	1360	1111	1271	1111	1414	1353
	100%	1404	1396	1391	1372	1136	1345	1303	1180	1039	761	761	1414	1232
C	Manual	1414	1414	1414	1413	1414	1414	1414	1398	1414	1398	1398	1414	1411
	20%	1414	1414	1414	1413	1292	1406	1367	1268	1330	1173	1173	1414	1349
	50%	1414	1414	1414	1411	1217	1381	1323	1200	1258	1044	1044	1414	1308
	100%	1410	1413	1412	1403	1082	1289	1208	1042	1121	797	797	1414	1218
D	Manual	1414	1414	1414	1414	1414	1414	1414	1267	1414	1407	1267	1414	1399
	20%	1414	1414	1414	1414	1390	1414	1414	1385	1321	1066	1066	1414	1365
	50%	1414	1414	1414	1414	1329	1412	1407	1335	1222	966	966	1414	1333
	100%	1412	1413	1414	1413	1203	1385	1367	1191	1101	684	684	1414	1258

W: Water, V: Vegetation, BS: Bare Soil, B: Building, and R: Road

4.2.3. Classes Homogeneity

Once various samples are chosen and checked statistically the signatures for the various samples are merged into the eight classes types as described. The properties of the training samples are tested, depending on the range of standard deviation. It is possible to discriminate homogeneity or heterogeneity of class in the training area. The lower standard deviation, the greater the homogeneity of the samples, and the higher standard deviation, the more heterogeneity of samples [16]. Table 2 shows training sample's statistical properties.

Fig. 6 shows the relation between the standard deviation of selected training samples and the percentage of histogram; 20%, 50%, and 100% of the area selected as training samples. The higher percentage of the area selected as training samples the higher standard deviation of the resulted signature. The higher standard deviation means that the signature represents great diversity which enhances results of classification.

TABLE 2. TRAINING SAMPLES STATISTICAL PROPERTIES OF STUDY AREA B.

	Water		Vegetation		Bare soil		Buildings		Roads	
	Mean	**Std. Dev.**	**Mean**	**Std. Dev.**	**Mean**	**Std. Dev.**	**Mean**	**Std. Dev.**	**Mean**	**Std. Dev.**
Manual samples	440.6	54.6	363.1	8.3	415.0	24.8	530.9	41.5	433.0	16.1
	335.4	66.9	227.5	9.1	293.8	28.4	419.4	46.6	300.4	16.5
	228.3	133.2	316.5	20.4	432.8	57.6	663.0	91.7	396.2	52.2
	742.7	279.7	341.9	32.6	613.9	90.5	960.6	140.6	521.3	47.9
	510.6	230.7	216.4	29.2	473.0	77.0	746.6	115.0	388.3	41.2
	647.7	217.1	745.1	117.1	677.8	106.4	956.8	140.9	503.7	54.0
	609.4	218.7	1053.1	173.9	668.3	108.9	875.5	132.2	460.5	56.7
	515.8	147.3	950.5	153.3	620.5	104.5	798.8	118.9	428.8	57.2
20% Automatic samples	375.3	14.9	369.5	15.9	418.3	44.9	513.6	42.2	432.8	45.1
	248.8	19.4	235.5	15.8	286.9	44.8	404.3	44.3	307.5	50.5
	332.4	49.9	304.5	84.4	311.8	158.4	629.9	96.6	374.1	106.4
	396.5	82.8	373.4	48.6	554.6	141.2	915.9	132.6	540.2	134.8
	261.1	61.9	245.9	43.0	400.4	118.4	723.6	98.2	417.9	128.7
	266.2	54.9	686.6	104.7	685.2	166.0	922.2	128.8	545.7	169.9
	199.4	34.0	916.3	127.2	724.4	181.1	865.9	115.7	520.3	203.2
	166.9	32.0	838.3	112.4	657.0	164.3	785.9	114.5	460.4	176.7
50% Automatic samples	372.7	16.7	372.0	19.3	420.6	46.7	502.4	43.9	435.1	44.9
	245.1	20.8	237.9	19.8	290.9	47.1	390.1	47.0	309.1	50.7
	320.7	48.4	307.6	86.8	316.0	157.8	598.8	100.9	380.3	113.3
	382.3	85.4	381.4	62.4	560.3	143.6	868.3	143.1	553.6	137.2
	250.2	63.6	253.1	57.5	414.3	124.7	681.9	110.0	426.0	128.8
	262.3	67.7	701.3	111.0	684.0	169.3	875.4	139.8	560.3	166.1
	203.1	51.0	921.7	167.3	719.2	187.9	820.3	129.1	531.1	195.8
	173.3	55.2	845.7	144.7	656.4	171.6	748.3	122.6	475.6	171.0
100% Automatic samples	377.2	29.6	382.7	31.3	426.1	48.2	470.6	48.9	443.5	45.5
	250.4	35.5	249.9	33.1	299.4	50.4	349.8	55.4	317.5	52.0
	315.7	60.4	303.9	110.4	345.4	155.0	505.0	130.0	411.8	122.1
	401.5	133.8	419.1	97.5	583.1	152.7	728.9	176.9	594.8	146.0
	264.7	103.6	292.4	96.8	442.7	136.1	562.3	146.4	453.9	129.5
	288.0	129.3	692.6	126.3	687.5	174.5	738.6	179.6	598.4	157.8
	229.4	119.0	865.0	209.4	712.0	193.8	689.9	176.0	559.3	174.3
	199.3	120.3	799.1	182.6	652.5	177.9	637.1	161.4	510.2	154.9

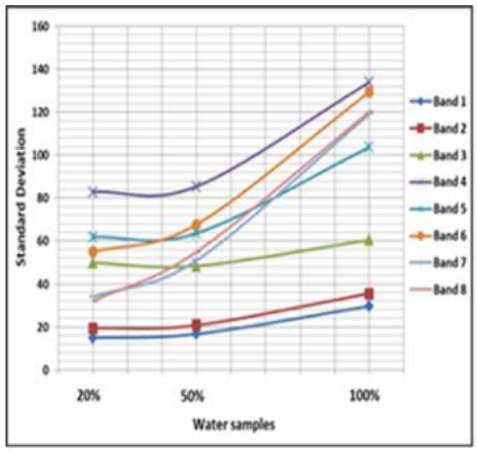

(a) Water standard deviation

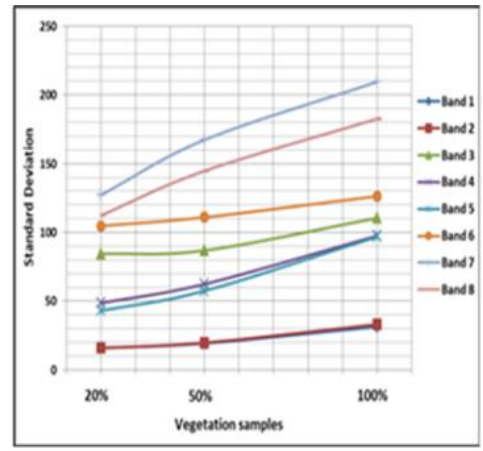

(b) Vegetation standard deviation

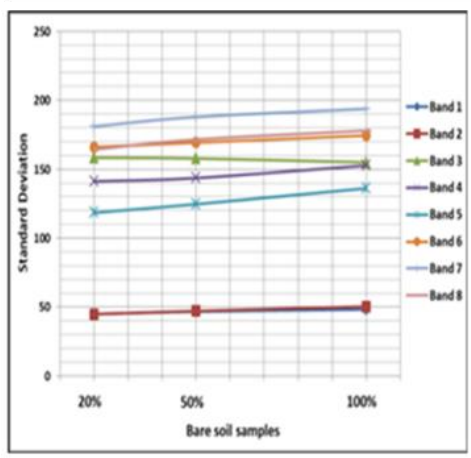

(c) Bare soil standard deviation

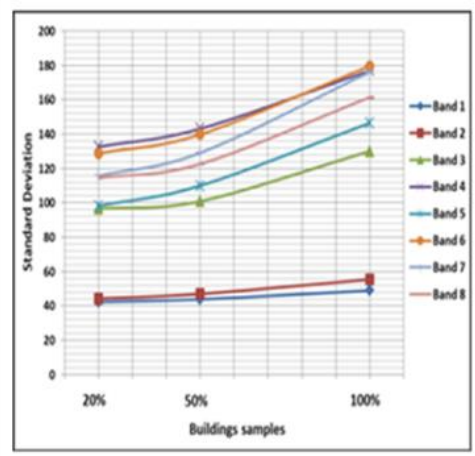

(d) Building standard deviation

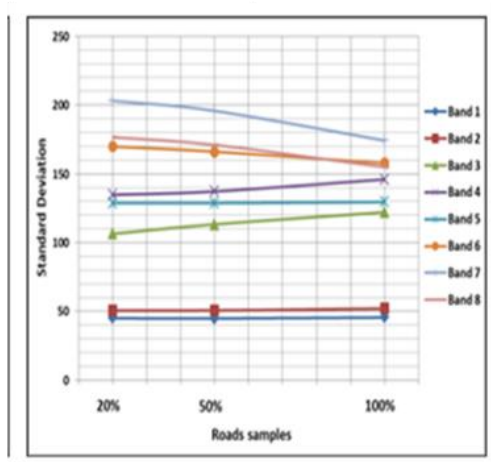

(e) Road standard deviation

Fig. 6. Training samples standard deviation, study area B.

5. RESULTS AND DISCUSSION

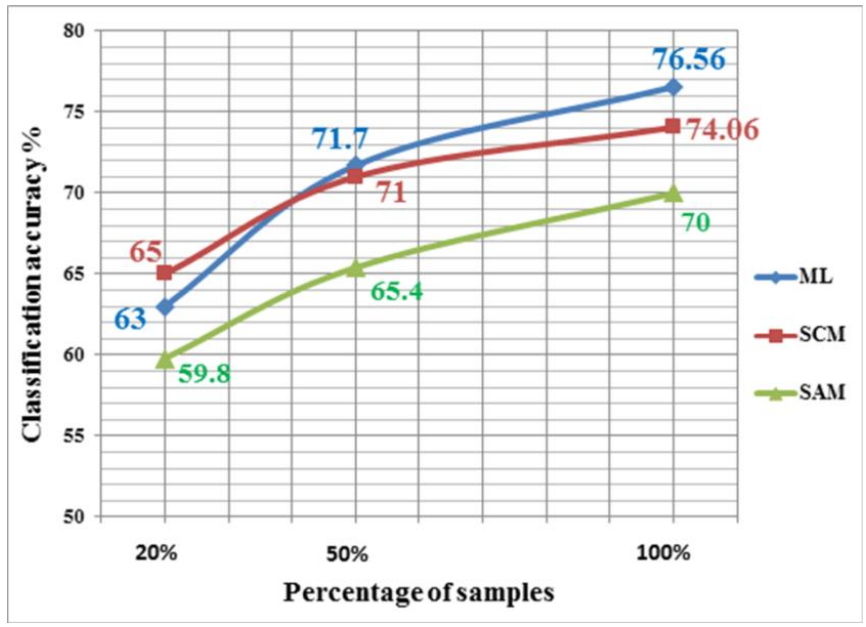

Fig. 7. The relation between percentage of samples and the classification accuracy.

A series of test images are used to validate the proposed method for the automatic selection of training samples. In the experiments, the proposed method is compared with the traditional method (i.e., manually collected samples), in order to verify the feasibility of the automatically selected samples [1]. The proposed method for samples selection is evaluated on a set of VHR satellite images over urban areas in the Egyptian environment and compared with classification using manually training samples. The visual results show that it is possible to automatically select candidate training samples. Fig.7 represents the relation between the area percentage of selected samples (20%, 50%, and 100%) and the classification accuracy for standard image classification methods (maximum likelihood, spectral angle mapper, and spectral correlation mapper). It is noted that the highest accuracy of classification can be achieved using 100% class as training samples for the three classification methods.

A series of test images are used to validate the proposed method for the automatic selection of training samples. In the experiments, the proposed method is compared with the traditional method (i.e., manually collected samples), in order to verify the feasibility of the automatically selected samples [1]. The proposed method for samples selection is evaluated on a set of VHR satellite images over urban areas in the Egyptian environment and compared with classification using manually training samples. The visual results show that it is possible to automatically select candidate training samples. Fig.7 represents the relation between the area percentage of selected samples (20%, 50%, and 100%) and the classification accuracy for standard image classification methods (maximum likelihood, spectral angle mapper, and spectral correlation mapper). It is noted that the highest accuracy of classification can be achieved using 100% class as training samples for the three classification methods.

The experiments with four test study areas; A, B, C, and D, showed that the proposed automatic training sample selecting method can achieve satisfactory classification accuracies (Fig. 8). Which are very close to the results obtained by the manually selected samples, with the most three commonly used classifiers as shown in Table 3 and Fig. 9.

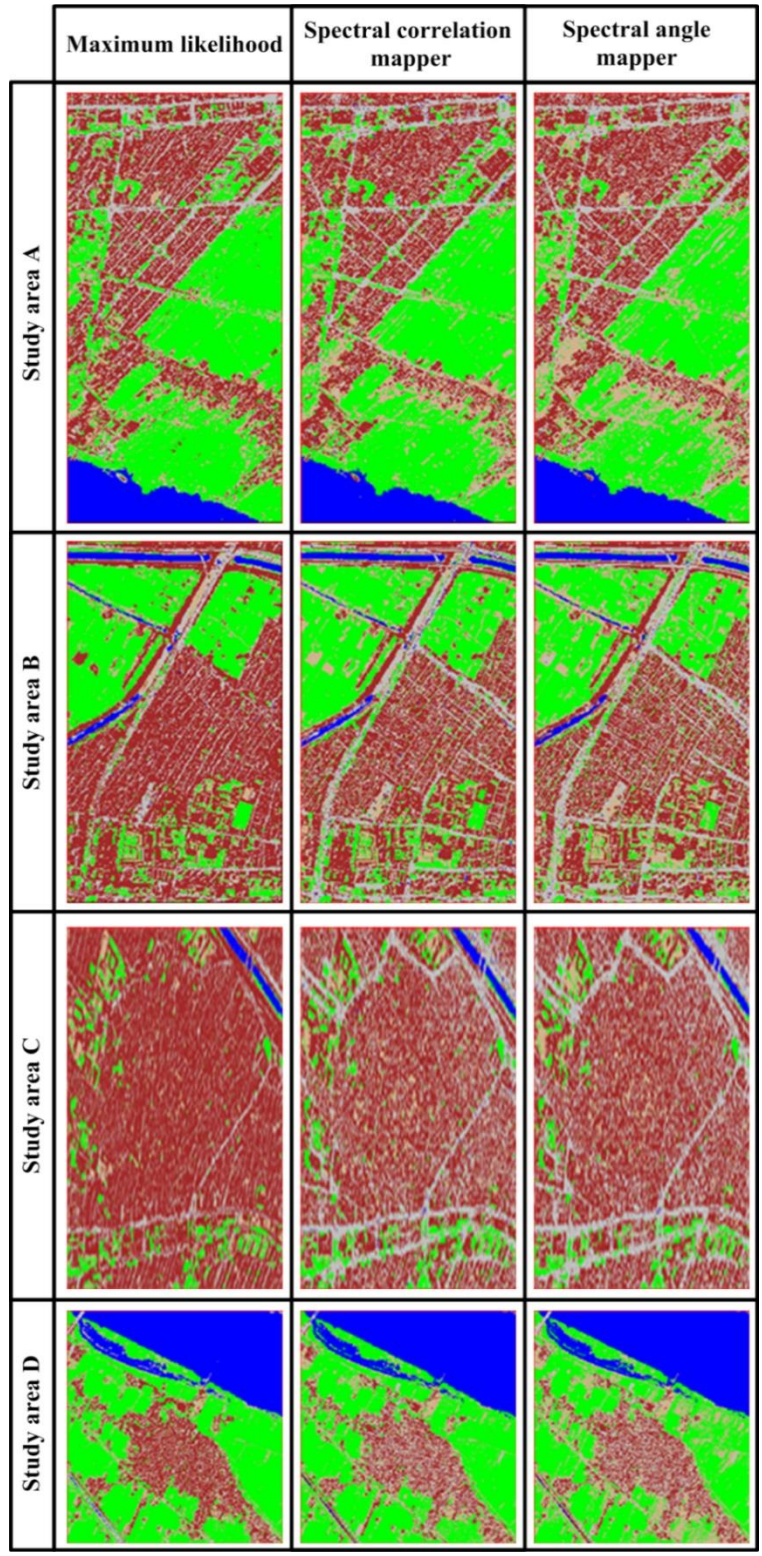

Fig. 8. Results of classification using automatic training samples.

TABLE 3. ACCURACIES OF CLASSIFICATION METHODS WITH MANUAL AND AUTOMATIC TRAINING SAMPLES.

Samples	Classification method	Overall accuracy %				
		Study area A	Study area B	Study area C	Study area D	Avg
Manual	Maximum likelihood	79.00	74.00	77.00	83.00	78.30
	Spectral correlation mapper	76.75	71.75	73.00	84.50	76.50
	Spectral angle mapper	68.50	68.50	68.75	67.00	73.75
100% Automatic	Maximum likelihood	81.50	68.75	75.75	80.25	76.56
	Spectral correlation mapper	81.00	65.25	72.25	77.75	74.06
	Spectral angle mapper	76.00	60.25	70.25	73.50	70.00

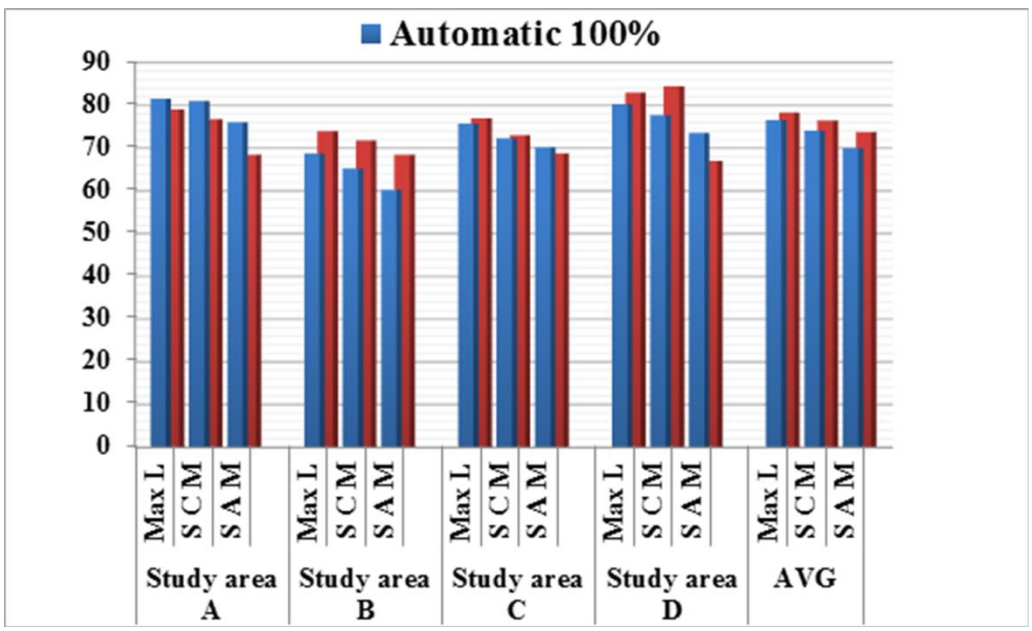

Fig. 9. Accuracies of classification methods with manual and automatic training samples.

The average accuracy achieved by the proposed automatic samples is acceptable (68.75% to 81.50%) for maximum likelihood classifier, (65.25% to 81.00%) for spectral correlation mapper classifier, and (60.25% to 76.00%) for spectral angle mapper classifier. Their accuracy scores are slightly nearby the manually selected samples by an average of 1.74% for maximum likelihood, 2.44% for spectral correlation mapper, and 3.75% for spectral angle mapper.

6. CONCLUSION

In this paper, an automatic method for selecting training samples from VHR satellite images for image classification is proposed. The method was evaluated and compared with manual training samples classification by three standard classification methods (Maximum likelihood, Spectral correlation mapper, and Spectral angle mapper). Results of this comparison demonstrate that classification accuracies obtained by the proposed automatic sampling method are very promising.

REFERENCES

[1] X. Huang, C. Weng, Q. Lu, T. Feng, and L. Zhang, "Automatic labelling and selection of training samples for high-resolution remote sensing image classification over urban areas," *Remote sensing*, vol. 7, pp. 16024-16044, 2015.

[2] Faten, Y. Mostafa, M. A. Yousef, and Y. A. Abas, "Using of high resolution satellite images for updating large scale mapping in Egypt," *J. Eng. Sci*, vol. 42, pp. 1122-1137, 2014.

[3] C. Li, J. Wang, L. Wang, L. Hu, and P. Gong, "Comparison of classification algorithms and training sample sizes in urban land classification with Landsat thematic mapper imagery," *Remote sensing*, vol. 6, pp. 964-983, 2014.

[4] G. M. Foody and A. Mathur, "The use of small training sets containing mixed pixels for accurate hard image classification: Training on mixed spectral responses for classification by a SVM," *Remote sensing of environment*, vol. 103, pp. 179-189, 2006.

[5] G. M. Foody, "The significance of border training patterns in classification by a feedforward neural network using back propagation learning," *International Journal of Remote Sensing*, vol. 20, pp. 3549-3562, 1999.

[6] R. Bardhan, R. Debnath, and S. Bandopadhyay, "A conceptual model for identifying the risk susceptibility of urban green spaces using geo-spatial techniques," *Modeling Earth Systems and Environment*, vol. 2, p. 144, 2016.

[7] T. G. Van Niel, T. R. McVicar, and B. Datt, "On the relationship between training sample size and data dimensionality: Monte Carlo analysis of broadband multi-temporal classification," *Remote sensing of environment*, vol. 98, pp. 468-480, 2005.

[8] M. Fawzy, Y. Mostafa, and F. Khodary, "AUTOMATIC INDICES BASED CLASSIFICATION METHOD FOR MAP UPDATING USING VHR SATELLITE IMAGES," *JES. Journal of Engineering Sciences*, vol. 48, pp. 845-868, 2020.

[9] Faten, Y. Mostafa, and M. A. Yousef, "THE OPTIMAL METHOD FOR CLASSIFYING HIGH RESOLUTION SATELLITE IMAGES IN EGYPT ENVIRONMENT," *J. Eng. Sci*, vol. 42, pp. 1106–1121, 2014.

[10] Y. Mostafa and A. Abdelhafiz, "Shadow identification in high resolution satellite images in the presence of water regions," *Photogrammetric Engineering & Remote Sensing*, vol. 83, pp. 87-94, 2017.

[11] P. Sarabandi, F. Yamazaki, M. Matsuoka, and A. Kiremidjian, "Shadow detection and radiometric restoration in satellite high resolution images," in *IGARSS 2004. 2004 IEEE International Geoscience and Remote Sensing Symposium*, 2004, pp. 3744-3747.

[12] N. Otsu, "A threshold selection method from gray-level histograms," *IEEE transactions on systems, man, and cybernetics*, vol. 9, pp. 62-66, 1979.

[13] J. B. Campbell and R. H. Wynne, *Introduction to remote sensing*: Guilford Press, 2011.

[14] A. Farrag and Y. Mostafa, "Comparison of Land Cover Change Detection Techniques with Satellite Images: Case Study in Assiut, Egypt," *Civil Engineering Research Magazine, Al-Azhar University*, vol. 28, pp. 983-996, 2006.

[15] J. Richards, "Remote Sensing Digital Image Analysis," ed, 2013, pp. 99-125.

[16] Y. Mostafa, ""Comparison of Land Cover Change Detection Methods Using SPOT Images". M.SC Thesis civil Engineering Dept., Assiut University Egypt.," 2006.